High-Accuracy Standard Specimens for the Line-Focus-Beam Ultrasonic Material Characterization System

Jun-ichi Kushibiki, *Member, IEEE*, Mototaka Arakawa, *Member, IEEE*, and Ryoichi Okabe

Abstract—**We prepared standard specimens for the line-focus-beam ultrasonic material characterization system to obtain absolute values of the propagation characteristics (phase velocity and attenuation) of leaky surface acoustic waves (LSAWs). The characterization system is very useful for evaluating and analyzing specimen surfaces. The calibration accuracy of these acoustic parameters depends on the accuracy of acoustical physical constants (elastic constants, piezoelectric constants, dielectric constants, and density) determined for standard specimens. In this paper, we developed substrates of nonpiezoelectric single crystals (viz., gadolinium gallium garnet [GGG], Si, and Ge) and an isotropic solid (synthetic silica [SiO_2] glass) as standard specimens. These specimens can cover the phase velocity range of 2600 to 5100 m/s for Rayleigh-type LSAWs. To determine the elastic constants with high accuracy, we measured velocities by the complex-mode measurement method and corrected diffraction effects. Measurements of bulk acoustic properties (bulk wave velocity and density) were conducted around 23°C, and bulk wave velocities were obtained with an accuracy of within ±0.004%. We clearly detected differences in acoustic properties by comparing the obtained results with the previously published values; the differences were considered to be due to differences of the specimens used. We also detected differences in acoustic properties among four SiO_2 substrates produced by different manufacturers.**

I. Introduction

We developed the line-focus-beam ultrasonic material characterization (LFB-UMC) system [1], [2]. The system evaluates and analyzes materials with high accuracy by measuring the propagation characteristics (viz., phase velocity and propagation attenuation) of leaky surface acoustic waves (LSAWs) excited and propagated on the surface of water-loaded specimens. This system has been applied to evaluate bulk materials such as $LiNbO_3$ and $LiTaO_3$ single crystals, and glasses, thin-film materials, and fabrication processes of electronic devices, successfully demonstrating its usefulness [1]–[30].

We intensively investigated its relative and absolute measurement accuracy. A relative accuracy of ±0.002% at a single chosen point and of ±0.004% in a two-dimensional inspection area of 200 mm × 200 mm were attained by developing stable electrical circuits and high-precision mechanical systems, stabilizing temperature environments, and measuring the water couplant temperature with high accuracy [2]. However, the use of different ultrasonic devices and different frequencies in measurements could result in significant differences in measured values of propagation characteristics obtained [31]. Because of this, the system must be calibrated when the absolute values of LSAW propagation characteristics need to be obtained, as in determining elastic constants using the LFB-UMC system [6], [10], [23]–[26], [32], [33]. For this purpose, we proposed a system calibration method using standard specimens [31], [34]. The system is calibrated by measuring acoustical physical constants (elastic constants, piezoelectric constants, dielectric constants and density) for standard specimens, and comparing measured values of LSAW propagation characteristics with the theoretical ones calculated using the constants determined. Therefore, it is important in this method to measure the acoustical physical constants precisely. Recently, we investigated the complex-mode measurement method in bulk wave velocity measurements. We also investigated a method to correct diffraction effects in velocity measurements and demonstrated that velocity values with nearly six significant figures can be obtained in the very high frequency (VHF) range [35]. This accuracy will contribute greatly to preparing standard specimens with higher accuracy.

This paper describes highly accurate measurements of acoustic properties of three nonpiezoelectric single crystals (gadolinium gallium garnet [GGG], Si, and Ge) and an isotropic solid (synthetic silica [SiO_2] glass) as standard specimens. Bulk acoustic properties of longitudinal and shear wave velocities, and densities are measured for the specimens around room temperatures, and their elastic constants and temperature dependences are obtained.

Manuscript received August 1, 2001; accepted December 7, 2001. This work was supported in part by Research Grants-in-Aid from the Ministry of Education, Science and Culture of Japan, from the Japan Society for the Promotion of Science for the Research for the Future Program, and by the Proposal-Based New Industry Creative-type Technology R&D Promotion Program from the New Energy and Industrial Technology Development Organization (NEDO) of Japan.

The authors are with the Department of Electrical Engineering, Tohoku University, Sendai 980-8579, Japan (e-mail: kushi@ecei.tohoku.ac.jp).

II. Bulk Acoustic Properties

For nonpiezoelectric materials, the elastic constant c is, in general, related to the density ρ and the velocity V in the following equation:

$$c = \rho V^2. \tag{1}$$

An isotropic solid, such as SiO_2 glass, has two independent elastic constants, c_{11} for longitudinal waves and c_{44} for shear waves. Nonpiezoelectric cubic crystals, such as GGG, Si, and Ge, have three independent elastic constants, c_{11}, c_{12}, and c_{44}. These three elastic constants can be determined accurately by measuring the [100]-propagating longitudinal velocity $V_{\ell[100]}$ and shear velocity $V_{s[100]}$, the [111]-propagating longitudinal velocity $V_{\ell[111]}$, and the density, and using the following equations [31]:

$$c_{11} = \rho V_{\ell[100]}^2, \tag{2}$$

$$c_{44} = \rho V_{s[100]}^2, \text{ and} \tag{3}$$

$$c_{11} + 2c_{12} + 4c_{44} = 3\rho V_{\ell[111]}^2. \tag{4}$$

III. Measuring Methods

To accurately determine the elastic constants, we must measure the velocity and density with high accuracy. The methods of measuring these parameters are as follows.

A. Bulk Wave Velocities

The velocity of bulk waves is obtained by measuring the amplitude and phase of radio frequency (RF) tone burst signals in the composite ultrasonic transmission line using the complex-mode measurement method. The measurement method and system are described in detail elsewhere [35]. The experimental arrangement is illustrated in Fig. 1. The plane-wave ultrasonic device employed here consists of a cylindrical buffer rod of synthetic SiO_2 glass with a transducer fabricated on one end of the rod. A ZnO piezoelectric film transducer made by DC diode sputtering [36] was used for the longitudinal wave measurement, and an X-cut $LiNbO_3$ transducer bonded to the rod, for the shear wave measurement. Coupling materials are pure water for longitudinal waves and salol (phenyl salicylate) for shear waves. Salol bonds the buffer rod and a specimen with a thickness of less than 1 μm, typically 0.2 to 0.5 μm.

In the longitudinal wave velocity measurements, a pure water layer is established with a certain distance, here typically 0.8–1.0 mm, between the SiO_2 buffer rod and the specimen, so the reflected pulse signals from the buffer rod end, V_1, can be separated from the reflected pulse signals from the front surface (V_2) and back surface (V_3) of the specimen in the time domain. By measuring the phase shift of V_3/V_2, ϕ, and the thickness of the specimen h, we obtain the bulk wave velocity of the specimen, V_ℓ, by the following equation:

$$V_\ell = -\frac{2\omega h}{\phi - \pi - \Delta\theta}, \tag{5}$$

where ω is the angular frequency, and $\Delta\theta$ is the difference between the phase advances of signals V_2 and V_3 caused by diffraction.

In the shear wave velocity measurements, additional phase shift occurs when shear waves transmit through or reflect on the bonding layer because V_1 signals cannot be separated from V_2 signals in the time domain. The effect of this phase shift, θ_{BL}, on the velocity measurement must be corrected. θ_{BL} is contained in the phase shift ϕ to be measured. It can be calculated using the acoustic parameters (velocity, attenuation coefficients, and density) of the bonding layer and by estimating the layer thickness by comparing measured and calculated frequency dependences of the reflection coefficient at the boundary between the SiO_2 buffer rod and the bonding layer. Thus, the shear wave velocity is given by

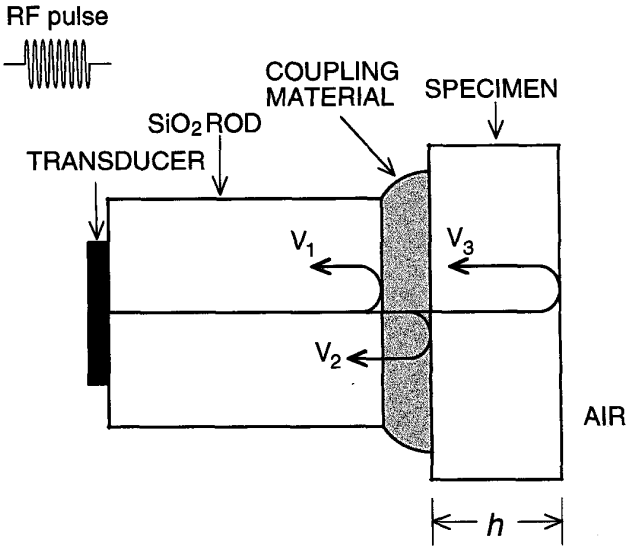

Fig. 1. Experimental arrangement for bulk velocity measurements of solid specimens using bulk ultrasonic RF pulses.

$$V_s = -\frac{2\omega h}{\phi - \pi - \Delta\theta - \theta_{BL}}. \tag{6}$$

To obtain accurate velocity, effects of diffraction must be corrected. $\Delta\theta$ is corrected through numerical calculations using the exact integral expression of diffraction [35], [37]. This expression is applied to calculate diffraction in a homogeneous medium during the propagation of longitudinal waves. Diffraction in an isotropic solid during the propagation of shear waves was reported to be approximately the same as that of longitudinal waves when ka (k, wave number; a, transducer radius) was larger than 100 [38]. As this condition applies to the measurements in this paper, diffraction during the propagation of shear waves is corrected with the same method as that of longitudinal waves. It also was reported that diffraction in an anisotropic solid is equal to that in an isotropic solid using the distance multiplied by (1–2b), where b is the anisotropy parameter [39]. For [100]- and [111]-propagating longitudinal waves in crystals belonging to the cubic system, b is given by the following equations in the literature [40]. For [100] propagation:

$$b = \frac{(c_{11} - c_{12} - 2c_{44})(c_{11} + c_{12})}{2c_{11}(c_{11} - c_{44})}. \tag{7}$$

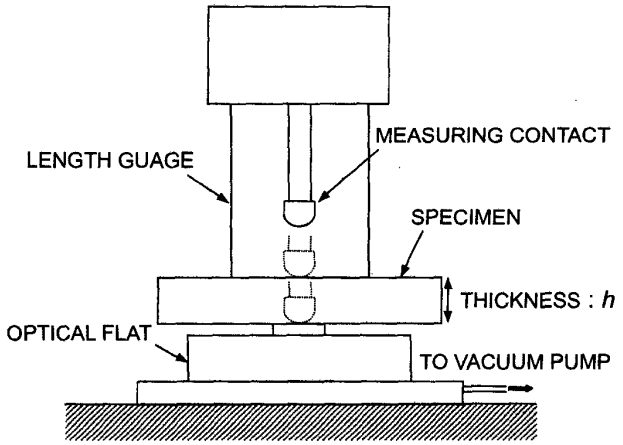

Fig. 2. Schematic view of the digital length gauging system.

For [111] propagation:

$$b = \frac{2\left(-c_{11}+c_{12}+2c_{44}\right)\left(c_{11}+2c_{12}+c_{44}\right)}{3\left(c_{12}+c_{44}\right)\left(c_{11}+2c_{12}+4c_{44}\right)}. \tag{8}$$

It is important to measure the thickness of the specimens precisely because the measurement accuracy of bulk wave velocities depends mainly on the measurement accuracy of the specimen thickness. Thickness is measured by a contacting method with a digital length gauging system with an optical encoder (CERTO CT2501, DR. JOHANNES HEIDENHAIN GmbH, Traunreut, Germany). The resolution of the gauging system is ± 0.005 μm. To ensure a stabilized measurement environment, the gauging system is placed on a vibration isolation system in a temperature-controlled chamber, in which the temperature is controlled at 23$\pm$0.1°C. Fig. 2 shows a schematic view of the gauging system. To reduce measurement errors caused by slight warps of the specimen surface, a special optical flat modified with a circular disk post of 8-mm diameter and 50-μm height formed by etching, as shown in Fig. 2, was devised so that the area contacting the specimen was reduced. The optical flat is securely fastened to a base plate of the gauging system by a vacuum pump. The reproducibility of the measurement is approximately ± 0.02 μm. In these measurements, strain might occur when the measuring contact touches the optical flat or the specimen and that may result in erroneous measurement values. To prevent this, we must consider the strain δ_{ij} introduced by the Hertzian contact, which is expressed in the following equation [41]:

$$\delta_{12} = \sqrt[3]{\frac{9}{16}\frac{1}{R_0}\left(\frac{1-\sigma_1^2}{E_1}+\frac{1-\sigma_2^2}{E_2}\right)^2 P^2}, \tag{9}$$

where R_0 is the curvature radius of the head of the measuring contact, σ_i is the Poisson ratio, E_i is Young's modulus, and P is the measurement force. Subscripts 1 and 2 denote the measurement contact and the optical flat or the specimen measured, respectively. When the material of the optical flat differs from that of the specimen to be measured, we should introduce the correction $\Delta\delta_{23}$ defined as $\delta_{12} - \delta_{13}$, where the subscripts 2 and 3 denote the optical flat and the specimen, respectively. It is easy to understand that $\Delta\delta_{23}$ is equal to zero when the materials are the same. The true thickness h is obtained by subtracting $\Delta\delta_{23}$ from the measured value h', as shown in the following equation:

$$h = h' - \Delta\delta_{23}. \tag{10}$$

However, it should be noted that, as (9) holds only for isotropic solids, strain for anisotropic solids was approximated assuming that they were isotropic solids. This method has been evaluated through experiments with various combinations of specimens and optical flats of different materials, and the findings have shown that the error introduced by the assumption is about ± 0.04 μm. In addition, for several standard gauge blocks (Class K [accuracy: ± 0.04 μm], Mitsutoyo Co., Kawasaki, Japan), practical standards of length[1] have been measured to confirm the accuracy of the digital length gauging system. We conclude from the above that, using an optical flat of synthetic silica glass, the thickness of an isotropic specimen is measured with an accuracy of ± 0.06 μm, and that of an anisotropic specimen, ± 0.10 μm obtained by adding the error of ± 0.04 μm due to the anisotropy factor.

B. Density

The density is determined by the Archimedes principle by weighing the specimen both in air and in water and using the following equation[2] [42]:

$$\rho = \frac{W_{\mathrm{A}}}{W_{\mathrm{A}}-W_{\mathrm{W}}}\rho_{\mathrm{W}} - \frac{W_{\mathrm{W}}}{W_{\mathrm{A}}-W_{\mathrm{W}}}\rho_{\mathrm{A}}, \tag{11}$$

where W_{A} and W_{W} are the weights in air and water, and ρ_{A} and ρ_{W} are the densities of air and water.

W_{A} and W_{W} are measured with an electronic balance (R160P, Sartorius Co., Goettingen, Germany). ρ_{A} and ρ_{W} are obtained from the literature [43], [44] at the measured temperature, barometric pressure and humidity for the measurement of the weight in air and in water. To reduce the influence of vibration, the electronic balance is placed on a very heavy and firm table made of stone. To further improve the measurement environment, the balance and table are placed in a temperature-controlled room, so that the density at an arbitrary temperature around the room temperature can be measured in a stabilized temperature environment. With this system and environment employed in the measurement, the uncertainty of the density of the

[1] Japanese Industrial Standards Committee, "Gauge blocks," JIS B 7506, Oct. 20, 1997.

[2] As no information on the influence of buoyancy of air was given in the density measurement manual by Sartorius, the experimental data we reported prior to 1995 [6], [12]–[13], [17], [34] must be corrected for this effect. The data can be corrected to four significant figures by substituting them into the equation of $(1.170\times10^{-3}\rho - 1.167)$ kg/m^3 under our measurement conditions of temperature 23°C, humidity 40%, and average barometric pressure 996.3 hPa.

specimen measured due to the errors of the densities of air and water is estimated to be less than ±0.002%, and the major error factor is the variations of the weight values measured in water.

IV. Specimens

Substrates with two basic crystalline surfaces of (100) and (111) were prepared as standard specimens from ingots of GGG (Czochralski [CZ] method, Shin-Etsu Chemical Co., Ltd., Tokyo, Japan), Si (floating zone [FZ] method, N-type (P), ≥1000 Ω·cm, Shin-Etsu Chemical Co., Ltd., Tokyo, Japan), and Ge (CZ method, nondoped, 50 Ω·cm, Tokyo Denshi Yakin Co., Ltd., Chigasaki, Japan). The (111) substrates were prepared with a larger size suitable for accurate density measurements. Synthetic silica glass substrates, produced by direct hydrolyzation of silicon tetrachloride ($SiCl_4$), by four different manufacturers (T-4040, Toshiba Ceramics Co., Ltd., Tokyo, Japan; C-7980, Corning Inc., Corning, NY; P-10, Shin-Etsu Quartz Products Co., Ltd., Tokyo, Japan; and N-ES, Nippon Silica Glass Co., Ltd., Yamagata, Japan) were prepared. Each specimen was optically polished on both sides. The parallelism is within 4 seconds, and its effect on velocity measurement is negligible.

As the specimen thickness increases, its measurement error has less influence on the accuracy of measured velocity, assuming that specimen material is sufficiently homogeneous. However, the effect of diffraction increases as the wave propagation length increases, and measurement errors also depend upon the RF pulse width and the intermediate frequency (IF) band width, typically 3 MHz, used in the measurement [35], [45]. Therefore, the specimen thicknesses were selected to be 5 to 11 mm under the established measurement conditions to have a pulse width of approximately 500 ns.

In measuring anisotropic media, inclination angles of the specimen surfaces from the crystalline surfaces result in errors in determining the constants. To avoid this, the crystalline surfaces of GGG, Si, and Ge specimens were examined by X-ray analysis. The results showed that the maximum inclination angle was 0.06°. Velocity changes caused by this inclination were investigated through numerical calculations and found to be less than 0.5 ppm for the longitudinal velocity and 1.0 ppm for the shear velocity, both of which were negligible.

V. Results

The bulk acoustic properties (V_ℓ, V_s, and ρ) were measured for the specimens described here. To obtain their temperature dependences, measurements were made at different temperatures, surrounding the specimen, at 20°C, 23°C, and 26°C. However, the densities of SiO_2 glass substrates were measured only at 23°C due to their very small density variations with the temperature difference of 3°C, ±0.01 kg/m^3. The specimen thicknesses were measured only at 23±0.1°C, and the thickness of each substrate at each temperature was obtained using the published values of the thermal expansion coefficients (6×10^{-6} for GGG[3], 2.3×10^{-6} for Si [46], 5.7×10^{-6} for Ge [46], and 0.52×10^{-6} for SiO_2[4]). The temperature variations during the bulk wave velocity measurement were within ±0.01°C. The temperature variations during the density and thickness measurements were within ±0.1°C. V_ℓ was measured at frequencies of 20 to 250 MHz, and V_s was measured at frequencies of 40 to 190 MHz. Considering the propagation length normalized by the Fresnel length [47] and signal-to-noise ratio (S/N) of the signals, the longitudinal velocities are the average values measured in the frequency range of 100 to 220 MHz, and the shear velocities in the frequency range of 130 to 170 MHz.

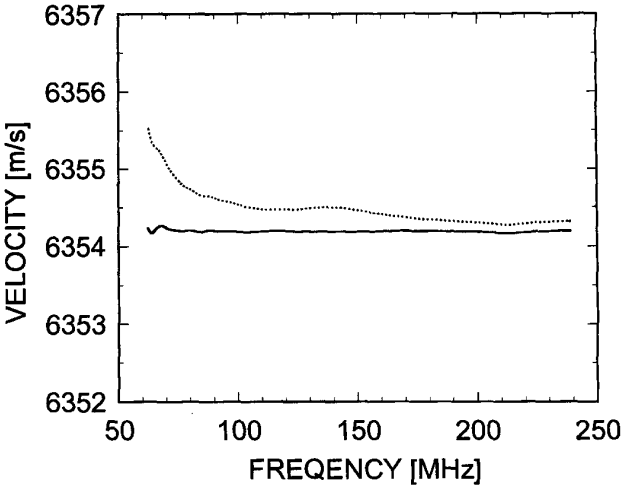

Fig. 3. Velocities for longitudinal waves on a (100) GGG specimen calculated from the measured phases in complex mode at 22.86°C. Dotted line, measured values. Solid line, diffraction corrected. The specimen thickness is 10639.68 μm.

Fig. 3 shows the measured results of the [100]-propagating longitudinal velocities for GGG. The measured values are plotted by the dotted line, and the values after the effect of diffraction was corrected are shown by the solid line. The measurements were made at 22.86°C. By correcting the diffraction effect, we obtain a velocity of 6354.19 (±0.03) m/s. Measured bulk acoustic velocities for GGG are shown in Fig. 4 as examples of the temperature dependences. The temperature coefficients were obtained by applying a linear approximation to the measured values using the least-squares method. The temperature dependences of both the longitudinal and shear velocities for GGG, Si, and Ge are negative; those of both the longitudinal and shear velocities for all of the SiO_2 specimens were positive. For GGG, Si, and Ge, the maximum differences between the measured values and values on the approximated straight lines were 0.03 m/s for the longitu-

[3]Technical Data, Shin-Etsu Chemical Co., Tokyo, Japan.
[4]Technical Data, Corning Inc., New York.

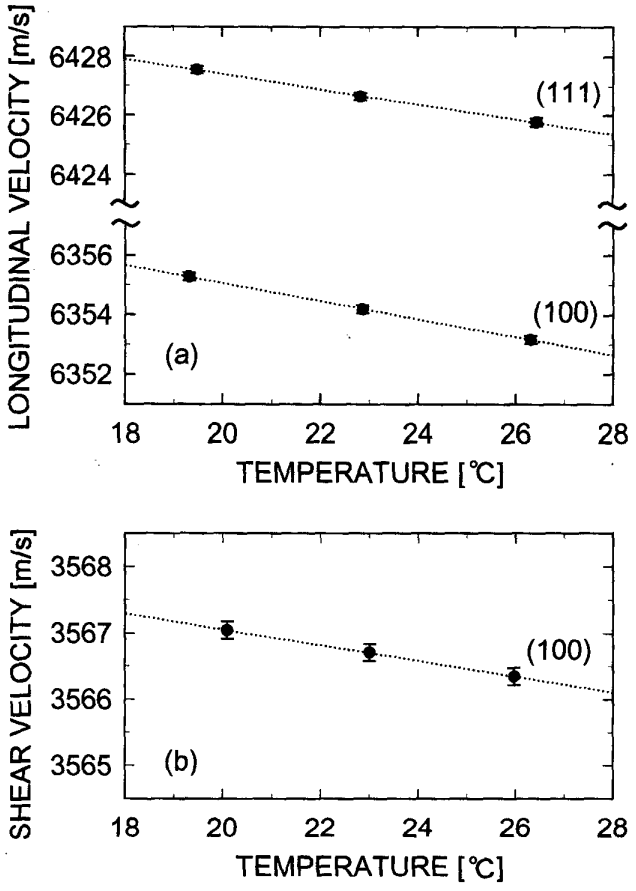

Fig. 4. Temperature dependences of bulk wave velocities for GGG specimens. Dots, measured. Dotted line, approximated.

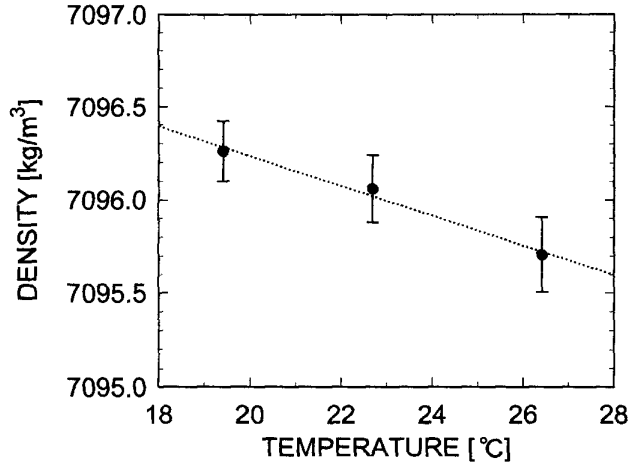

Fig. 5. Temperature dependence of density for GGG. Dots, measured. Dotted line, approximated.

dinal velocities and 0.01 m/s for the shear velocities. For SiO_2, they were 0.13 m/s for the longitudinal velocities and 0.02 m/s for the shear velocities. Fig. 5 shows the measured results of temperature dependences of densities for GGG, as an example. The temperature dependences of the densities obtained for GGG, Si, and Ge are all negative. The maximum differences between the measured values and values on the approximated straight lines were 0.04 kg/m^3 for GGG, 0.03 kg/m^3 for Si, and 0.02 kg/m^3 for Ge. Based on the above measured results, the bulk acoustic properties measured at 23°C are given in Table I, where α_{V_ℓ}, α_{V_s}, and α_ρ are the temperature coefficients of V_ℓ, V_s, and ρ, and the values in parentheses are measurement errors.

We obtained the elastic constants at 23°C from the measured results given here. Tables II, III, and IV give the results for GGG, Si, and Ge, and Table V gives those for SiO_2. The values of the constants of GGG published by Graham and Chang [48], and those of Si, Ge, and SiO_2 published by McSkimin [49] also are presented. In the tables, $\alpha_{c_{ij}}$ is the temperature coefficient of c_{ij}, and the values in parentheses are measurement errors. The temperature dependences of the elastic constants exhibited the same tendencies as those of the velocities and densities. However, as the GGG values of Graham and Chang [48] were taken at 25°C, the values at 23°C were obtained using the temperature coefficient value measured in these measurements. Also, as the published densities of Si and Ge were taken at 25°C, the densities at 23°C were obtained using the thermal expansion coefficients published previously [46].

VI. Discussions

In this paper, the measurement accuracy of bulk wave velocities is within ±0.003% for GGG, Si, and Ge, and within ±0.004% for SiO_2; the measurement accuracy of the density is within ±0.005%. The measurement accuracy of the elastic constants c_{11} and c_{44} for GGG, Si, and Ge is within ±0.015%, and that of c_{12} is within ±0.062%; the accuracy of c_{11} and c_{44} for SiO_2 is within ±0.013%. Those elastic constants were obtained with such higher accuracy that the determined values were very close to five significant figures. In contrast, for the standard specimens of GGG used previously, the accuracy was within ±0.011% in bulk wave velocities, ±0.033% in c_{11} and c_{44}, and ±0.12% in c_{12} [31].

Next, we compared the elastic constants of GGG, Si, and Ge determined here with those previously published by other researchers [48], [49]. The GGG values were compared with those of Graham and Chang [48]. The measurement accuracy of velocities was within 0.5%. The difference between our value of c_{12} determined here and their value is 0.7%. They compared the density of the specimen obtained by measuring the mass and volume with that obtained by measuring the lattice constant by X-ray analysis. The result showed that the former was over 0.1% less than

TABLE I

BULK ACOUSTIC PROPERTIES OF GGG, SI, GE CRYSTALS, AND SiO_2 GLASSES AT 23°C.

Specimen		h (μm)	V_ℓ (m/s)	α_{V_ℓ} ($\times 10^{-5}$/°C)	V_s (m/s)	α_{V_s} ($\times 10^{-5}$/°C)	ρ (kg/m^3)	α_ρ ($\times 10^{-5}$/°C)
GGG	(100)	10639.69 (±0.10)	6354.16 (±0.11)	−4.7	3566.70 (±0.12)	−3.3	7096.02 (±0.22)	−1.1
	(111)	10781.44 (±0.10)	6426.63 (±0.10)	−4.0	—	—		
Si	(100)	8399.50 (±0.10)	8432.41 (±0.15)	−3.3	5843.87 (±0.15)	−2.5	2328.89 (±0.12)	−1.2
	(111)	9374.78 (±0.10)	9355.38 (±0.15)	−3.1	—	—		
Ge	(100)	8303.42 (±0.10)	4913.49 (±0.11)	−4.5	3542.70 (±0.11)	−4.6	5326.16 (±0.28)	−1.0
	(111)	9348.63 (±0.10)	5552.04 (±0.11)	−4.5	—	—		
Synthetic silica glass	T-4040	5003.75 (±0.06)	5942.41 (±0.14)	12.1	3762.65 (±0.08)	7.6	2200.50 (±0.06)	—
	C-7980	4985.48 (±0.06)	5929.14 (±0.11)	12.8	3767.62 (±0.07)	8.2	2199.82 (±0.11)	—
	P-10	4971.10 (±0.06)	5930.75 (±0.17)	12.9	3767.90 (±0.07)	7.9	2200.02 (±0.09)	—
	N-ES	4936.47 (±0.06)	5927.34 (±0.25)	13.1	3761.65 (±0.07)	7.9	2200.15 (±0.07)	—

$V(T°C) = V(23°C) \times (1 + \alpha_V \Delta T)$ (m/s), $\rho(T°C) = \rho(23°C) \times (1 + \alpha_\rho \Delta T)$ (kg/m^3), $\Delta T = T - 23(°C)$.

TABLE II

DIFFERENCES IN ELASTIC CONSTANTS AND DENSITY BETWEEN MEASURED AND PUBLISHED [48] VALUES OF GGG AT 23°C.

	c_{11} ($\times 10^{11}$ N/m^2)	$\alpha_{c_{11}}$ ($\times 10^{-5}$/°C)	c_{12} ($\times 10^{11}$ N/m^2)	$\alpha_{c_{12}}$ ($\times 10^{-5}$/°C)	c_{44} ($\times 10^{11}$ N/m^2)	$\alpha_{c_{44}}$ ($\times 10^{-5}$/°C)	ρ (kg/m^3)	α_ρ ($\times 10^{-5}$/°C)
Measured	2.8650 (±0.0002)	−10.5	1.1582 (±0.0004)	−9.6	0.9027 (±0.0001)	−7.7	7096.02 (±0.22)	−1.1
Published	2.859		1.150		0.903		7094	
Difference	+0.006 (+0.2%)		+0.008 (+0.7%)		−0.000 (−0.0%)		+2 (+0.03%)	

$c_{ij}(T°C) = c_{ij}(23°C) \times (1 + \alpha_{c_{ij}} \Delta T)$ (N/m^2), $\Delta T = T - 23(°C)$.

TABLE III

DIFFERENCES IN ELASTIC CONSTANTS AND DENSITY BETWEEN MEASURED AND PUBLISHED [49] VALUES OF SI AT 23°C.

	c_{11} ($\times 10^{11}$ N/m^2)	$\alpha_{c_{11}}$ ($\times 10^{-5}$/°C)	c_{12} ($\times 10^{11}$ N/m^2)	$\alpha_{c_{12}}$ ($\times 10^{-5}$/°C)	c_{44} ($\times 10^{11}$ N/m^2)	$\alpha_{c_{44}}$ ($\times 10^{-5}$/°C)	ρ (kg/m^3)	α_ρ ($\times 10^{-5}$/°C)
Measured	1.6560 (±0.0001)	−7.8	0.6388 (±0.0003)	−9.9	0.7953 (±0.0001)	−6.2	2328.89 (±0.12)	−1.2
Published	1.657	−6.75	0.6390	−9.95	0.7956	−4.4	2331	
Difference	−0.001 (−0.1%)	−1.05 (−16%)	−0.0002 (−0.0%)	+0.05 (+1%)	−0.0003 (−0.0%)	−1.8 (−41%)	−2 (−0.09%)	

$c_{ij}(T°C) = c_{ij}(23°C) \times (1 + \alpha_{c_{ij}} \Delta T)$ (N/m^2), $\Delta T = T - 23(°C)$.

TABLE IV

DIFFERENCES IN ELASTIC CONSTANTS AND DENSITY BETWEEN MEASURED AND PUBLISHED [49] VALUES OF GE AT 23°C.

	c_{11} ($\times 10^{11}$ N/m^2)	$\alpha_{c_{11}}$ ($\times 10^{-5}$/°C)	c_{12} ($\times 10^{11}$ N/m^2)	$\alpha_{c_{12}}$ ($\times 10^{-5}$/°C)	c_{44} ($\times 10^{11}$ N/m^2)	$\alpha_{c_{44}}$ ($\times 10^{-5}$/°C)	ρ (kg/m^3)	α_ρ ($\times 10^{-5}$/°C)
Measured	1.2859 (±0.0001)	−10.0	0.4828 (±0.0003)	−9.5	0.6685 (±0.0001)	−10.2	5326.16 (±0.28)	−1.0
Published	1.289	−11.1	0.4831	−11.9	0.6710	−9.2	5323	
Difference	−0.003 (−0.2%)	+1.1 (+10%)	−0.0003 (−0.1%)	+2.4 (+20%)	−0.0025 (−0.4%)	−1.0 (−11%)	+3 (+0.06%)	

$c_{ij}(T°C) = c_{ij}(23°C) \times (1 + \alpha_{c_{ij}} \Delta T)$ (N/m^2), $\Delta T = T - 23(°C)$.

TABLE V
DIFFERENCES IN ELASTIC CONSTANTS AND DENSITY BETWEEN MEASURED AND PUBLISHED [49] VALUES OF SiO_2 AT 23°C.

Specimen	c_{11} ($\times 10^{10}$ N/m^2)	$\alpha_{c_{11}}$ ($\times 10^{-4}$/°C)	c_{44} ($\times 10^{10}$ N/m^2)	$\alpha_{c_{44}}$ ($\times 10^{-4}$/°C)	ρ (kg/m^3)
T-4040	7.7705 (±0.0006)	2.4	3.1154 (±0.0002)	1.5	2200.50
C-7980	7.7334 (±0.0007)	2.6	3.1226 (±0.0003)	1.6	2199.82
P-10	7.7383 (±0.0008)	2.6	3.1234 (±0.0003)	1.6	2200.02
N-ES	7.7299 (±0.0010)	2.6	3.1132 (±0.0003)	1.6	2200.15
Published	7.844	2.35	3.126	1.46	2203

$c_{ij}(T°C) = c_{ij}(23°C) \times (1 + \alpha_{c_{ij}} \Delta T)$ (N/m^2), $\Delta T = T - 23$(°C).

the latter; this difference was attributed to the voids in the specimen. This indicates that the differences between the measured and published values of the elastic constants may have been caused by the differences in the quality of the specimens and minute differences in their chemical composition ratios.

The Si and Ge values were compared with McSkimin's values [49]. His measurement accuracy of velocities was within 0.5%. For Si, there were almost no differences in the elastic constants, but a difference of about 0.1% in the density was observed, as well as a large difference in the temperature coefficient of c_{44}. For Ge, 0.4% difference is seen in c_{44} as well as 10–20% differences in the temperature coefficients. The elastic constants of Si and Ge, and their temperature coefficients, were reported to vary with the doping level of impurities [50]–[53]. We can deduce from this that the differences in the measured values are due to the differences in impurity concentration or in crystal quality arising from the different crystal growth methods (CZ and FZ) between the specimens used here and those used by McSkimin [49].

Differences in the elastic constants and density were detected among the SiO_2 substrates. SiO_2 is a glass of high purity with very little metallic impurity. However, hydroxyls and chlorine are incorporated into the material during the fabrication processes, and induce changes in their acoustic properties [27]. The different thermal histories during the fabrication processes also lead to differences in acoustic properties [54]. Therefore, we consider that the differences in the acoustic properties detected among the four substrates are due to the factors mentioned here.

VII. CONCLUDING REMARKS

This paper described the acoustic properties of GGG, Si, Ge single crystals and SiO_2 glasses as standard specimens for calibrating the LFB-UMC system, in which their elastic constants and densities were measured accurately at around 23°C. The complex mode measurement was used to measure bulk wave velocities, and the effect of diffraction was corrected. The measurement accuracy of velocities depends mainly upon the measurement accuracy of the specimen thickness, so a method for precisely measuring specimen thickness also was investigated. Improving the measurement environment enabled us to correct the effect of strain caused by the contact of the length gauging system. The absolute accuracy of the gauging system also was examined with standard gauge blocks. Through these efforts, we succeeded in very accurately measuring longitudinal and shear wave velocities as well as densities, and in determining the elastic constants with higher accuracy. Therefore, we could prepare more reliable standard specimens for the LFB system. We also compared the measured acoustical physical constants of each material with ones previously published by other researchers [48], [49] and observed some differences in values due to the different specimens used in the measurements. For SiO_2, we saw small but significant differences in the elastic constants and density among the four substrates used in these measurements. These differences were caused by different conditions during the fabrication processes.

The standard specimens developed can be used for calibrating the LFB-UMC system in the LSAW velocity range of 2600 to 5100 m/s. We can use all materials as standard specimens for the LFB-UMC system, if their acoustical physical constants can be determined. In principle, to obtain highly accurate absolute values of LSAW propagation characteristics, we must prepare individual standard specimens for each material to be characterized or substitute other standard specimens with almost the same velocities as each material to be evaluated. Recently, acoustical physical constants of $LiNbO_3$ and $LiTaO_3$ crystals [55] and synthetic α-quartz [56] have been precisely determined, and these have been used as standard specimens [32], [33].

ACKNOWLEDGMENTS

The authors are grateful to J. Hirohashi for analyzing the specimen surfaces by an X-ray diffractometer using the Bond method; M. Kawabuchi, Matsushita Communication Industrial Co. Ltd., Yokohama, Japan, for fabricating the shear ultrasonic devices used in the experiments; Y. Okada

of Kougakugiken Co. Ltd., Atsugi, Japan, for preparing the specimens; and Y. Shinozaki, Chuo Precision Co. Ltd., Tokyo, Japan, for his valuable cooperation in constructing the precise system for the thickness measurement.

REFERENCES

[1] J. Kushibiki and N. Chubachi, "Material characterization by line-focus-beam acoustic microscope," *IEEE Trans. Sonics Ultrason.*, vol. SU-32, pp. 189–212, Mar. 1985.

[2] J. Kushibiki, Y. Ono, Y. Ohashi, and M. Arakawa, "Development of the line-focus-beam ultrasonic material characterization system," *IEEE Trans. Ultrason., Ferroelect., Freq. Contr.*, vol. 49, pp. 99–113, Jan. 2002.

[3] J. Kushibiki and N. Chubachi, "Acoustic microscopy for materials characterization," in *Proc. Ultrason. Int. 91 Conf.*, 1991, pp. 1–13.

[4] K. Yamanaka, J. Kushibiki, and N. Chubachi, "Anisotropy detection in hot-pressed silicon nitride by acoustic microscopy using the line-focus beam," *Electron. Lett.*, vol. 21, pp. 165–167, Feb. 1985.

[5] P. J. Burnett, G. A. D. Briggs, S. M. Al-Shukri, J. F. Duffy, and R. M. De La Rue, "Acoustic properties of proton-exchanged $LiNbO_3$ studied using the acoustic microscopy $V(z)$ technique," *J. Appl. Phys.*, vol. 60, pp. 2517–2522, Oct. 1986.

[6] J. Kushibiki, T. Ueda, and N. Chubachi, "Determination of elastic constants by LFB acoustic microscope," in *Proc. IEEE Ultrason. Symp.*, 1987, pp. 817–821.

[7] J. Kushibiki and N. Chubachi, "Application of LFB acoustic microscope to film thickness measurements," *Electron. Lett.*, vol. 23, pp. 652–654, June 1987.

[8] C. K. Jen, C. Neron, J. F. Bussiere, L. Li, R. Lowe, and J. Kushibiki, "Characterization of cladded glass fibers using acoustic microscopy," *Appl. Phys. Lett.*, vol. 55, pp. 2485–2487, Dec. 1989.

[9] M. Obata, H. Shimada, and T. Mihara, "Stress dependence of leaky surface wave on PMMA by line-focus-beam acoustic microscope," *Exp. Mech.*, vol. 30, pp. 34–39, Mar. 1990.

[10] J. Kushibiki, T. Ishikawa, and N. Chubachi, "Cut-off characteristics of leaky Sezawa and pseudo-Sezawa wave modes for thin-film characterization," *Appl. Phys. Lett.*, vol. 57, pp. 1967–1969, Nov. 1990.

[11] J. Kushibiki, H. Takahashi, T. Kobayashi, and N. Chubachi, "Quantitative evaluation of elastic properties of $LiTaO_3$ crystals by line-focus-beam acoustic microscopy," *Appl. Phys. Lett.*, vol. 58, pp. 893–895, Mar. 1991.

[12] ——, "Characterization of $LiNbO_3$ crystals by line-focus-beam acoustic microscopy," *Appl. Phys. Lett.*, vol. 58, pp. 2622–2624, June 1991.

[13] J. Kushibiki, T. Kobayashi, H. Ishiji, and N. Chubachi, "Elastic properties of 5-mol % MgO doped $LiNbO_3$ crystals measured by line focus beam acoustic microscopy," *Appl. Phys. Lett.*, vol. 61, pp. 2164–2166, Nov. 1992.

[14] C. K. Jen, Z. Wang, A. Nicolle, C. Neron, E. L. Adler, and J. Kushibiki, "Acoustic graded-index lenses," *Appl. Phys. Lett.*, vol. 59, pp. 1398–1400, Sep. 1991.

[15] C. K. Jen, C. Neron, A. Shang, K. Abe, L. Bonnell, and J. Kushibiki, "Acoustic characterization of silica glasses," *J. Amer. Ceram. Soc.*, vol. 76, pp. 712–716, Mar. 1993.

[16] Y. Ono, J. Kushibiki, and N. Chubachi, "Characterization of optical fiber preforms by line-focus-beam acoustic microscopy," in *Proc. IEEE Ultrason. Symp.*, 1993, pp. 1243–1246.

[17] J. Kushibiki, H. Ishiji, T. Kobayashi, and T. Sasamata, "Characterization of 36°YX-$LiTaO_3$ wafers by line-focus-beam acoustic microscopy," *IEEE Trans. Ultrason., Ferroelect., Freq. Contr.*, vol. 42, pp. 83–90, Jan. 1995.

[18] A. Tourlog, J. D. Achenbach, and J. Kushibiki, "Line-focus acoustic microscopy measurements of acoustic properties of $LiTaO_3$ crystal plates with an inversion layer," *J. Appl. Phys.*, vol. 81, pp. 6616–6621, May 1997.

[19] J. Kushibiki, T. Kobayashi, H. Ishiji, and C. K. Jen, "Surface-acoustic-wave properties of MgO-doped $LiNbO_3$ single crystals measured by line-focus-beam acoustic microscopy," *J. Appl. Phys.*, vol. 85, pp. 7863–7868, June 1999.

[20] J. Kushibiki, Y. Ono, and I. Takanaga, "Ultrasonic microspectroscopy of $LiNbO_3$ and $LiTaO_3$ single crystals for SAW devices," *Trans. IEICE C-I*, vol. J82-C-I, pp. 715–727, Dec. 1999.

[21] J. Kushibiki, T. Okuzawa, J. Hirohashi, and Y. Ohashi, "Line-focus-beam acoustic microscopy characterization of optical-grade $LiTaO_3$ single crystals," *J. Appl. Phys.*, vol. 87, pp. 4395–4403, May 2000.

[22] J. Kushibiki, Y. Ohashi, and Y. Ono, "Evaluation and selection of $LiNbO_3$ and $LiTaO_3$ substrates for SAW devices by the LFB ultrasonic material characterization system," *IEEE Trans. Ultrason., Ferroelect., Freq. Contr.*, vol. 47, pp. 1068–1076, July 2000.

[23] T. Mihara and M. Obata, "Elastic constant measurement by using line-focus-beam acoustic microscope," *Exp. Mech.*, vol. 32, pp. 30–33, Mar. 1992.

[24] J. O. Kim, J. D. Achenbach, P. B. Mirkarimi, M. Shinn, and S. A. Barnett, "Elastic constants of single-crystal transition-metal nitride films measured by line-focus acoustic microscopy," *J. Appl. Phys.*, vol. 72, pp. 1805–1811, Sep. 1992.

[25] J. O. Kim, J. D. Achenbach, M. Shinn, and S. A. Barnett, "Effective elastic constants and acoustic properties of single-crystal TiN/NbN superlattices," *J. Mater. Res.*, vol. 7, pp. 2248–2256, Aug. 1992.

[26] Y. C. Lee, J. O. Kim, and J. D. Achenbach, "Acoustic microscopy measurement of elastic constants and mass density," *IEEE Trans. Ultrason., Ferroelect., Freq. Contr.*, vol. 42, pp. 253–264, Mar. 1995.

[27] J. Kushibiki, T. C. Wei, Y. Ohashi, and A. Tada, "Ultrasonic microspectroscopy characterization of silica glass," *J. Appl. Phys.*, vol. 87, pp. 3113–3121, Mar. 2000.

[28] J. Kushibiki, M. Miyashita, and N. Chubachi, "Quantitative characterization of proton-exchanged layers in $LiTaO_3$ optoelectronic devices by line-focus-beam acoustic microscopy," *IEEE Photon. Technol. Lett.*, vol. 8, pp. 1516–1518, Nov. 1996.

[29] J. Kushibiki and M. Miyashita, "Characterization of domain-inverted layers in $LiTaO_3$ by line-focus-beam acoustic microscopy," *Jpn. J. Appl. Phys.*, vol. 36, pp. 959–961, July 1997.

[30] ——, "Quantitative evaluation of fabrication processes of proton-exchanged layers in $LiTaO_3$ optoelectronic devices by the line-focus-beam ultrasonic material characterization system," *J. Appl. Phys.*, vol. 89, pp. 2017–2024, Feb. 2001.

[31] J. Kushibiki and M. Arakawa, "A method for calibrating the line-focus-beam acoustic microscopy system," *IEEE Trans. Ultrason., Ferroelect., Freq. Contr.*, vol. 45, pp. 421–430, Mar. 1998.

[32] I. Takanaga and J. Kushibiki, "A method of determining acoustical physical constants for piezoelectric materials by the line-focus-beam ultrasonic material characterization system," *IEEE Trans. Ultrason., Ferroelect., Freq. Contr.*, to be published.

[33] J. Kushibiki, I. Takanaga, S. Komatsuzaki, and T. Ujiie, "Chemical composition dependences of acoustical physical constants of $LiNbO_3$ and $LiTaO_3$ single crystals," *J. Appl. Phys.*, to be published.

[34] J. Kushibiki, T. Wakahara, T. Kobayashi, and N. Chubachi, "A calibration method of the LFB acoustic microscope system using isotropic standard specimens," in *Proc. IEEE Ultrason. Symp.*, 1992, pp. 719–722.

[35] J. Kushibiki and M. Arakawa, "Diffraction effects on bulk-wave ultrasonic velocity and attenuation measurements," *J. Acoust. Soc. Amer.*, vol. 108, pp. 564–573, Aug. 2000.

[36] N. Chubachi, "ZnO films for surface acoustooptic devices on nonpiezoelectric substrates," in *Proc. IEEE*, vol. 64, pp. 772–774, May 1976.

[37] A. O. Williams, Jr., "The piston source at high frequencies," *J. Acoust. Soc. Amer.*, vol. 23, pp. 1–6, Jan. 1951.

[38] D. H. Green and H. F. Wang, "Shear wave diffraction loss for circular plane-polarized source and receiver," *J. Acoust. Soc. Amer.*, vol. 90, pp. 2697–2704, Nov. 1991.

[39] M. G. Cohen, "Optical study of ultrasonic diffraction and focusing in anisotropic media," *J. Appl. Phys.*, vol. 38, pp. 3821–3828, Sep. 1967.

[40] E. P. Papadakis, "Ultrasonic diffraction loss and phase change in anisotropic materials," *J. Acoust. Soc. Amer.*, vol. 40, pp. 863–876, May 1966.

[41] K. L. Johnson, "Normal contact of elastic solids: Hertz theory," in *Contact Mechanics*. Cambridge: Cambridge Univ. Press, 1989, ch. 4, pp. 84–106.

[42] H. A. Bowman, R. M. Schoonover, and M. W. Jones, "Procedure for high precision density determinations by hydrostatic weighing," *J. Res. Natl. Bur. Stand.*, vol. 71C, pp. 179–198, July–Aug. 1967.
[43] R. S. Davis, "Equation for the determination of the density of moist air (1981/91)," *Metrologia*, vol. 29, pp. 67–70, 1992.
[44] F. E. Jones and G. L. Harris, "ITS-90 density of water formulation for volumetric standards calibration," *J. Res. Natl. Inst. Stand. Technol.*, vol. 97, pp. 335–340, May–June 1992.
[45] J. Kushibiki, T. Sannomiya, and N. Chubachi, "A useful acoustic measurement system for pulse mode in VHF and UHF ranges," *IEEE Trans. Sonics Ultrason.*, vol. SU-29, pp. 338–342, Nov. 1982.
[46] A. S. Bhala and E. W. White, "Coefficient of linear expansion of silicon and germanium by double crystal X-ray spectrometer," *Phys. Stat. Sol. (a)*, vol. 5, pp. K51–K53, Apr. 1971.
[47] H. Seki, A. Granato, and R. Truell, "Diffraction effects in the ultrasonic field of a piston source and their importance in the accurate measurement of attenuation," *J. Acoust. Soc. Amer.*, vol. 28, pp. 230–238, Mar. 1956.
[48] L. J. Graham and R. Chang, "Elastic moduli of single-crystal gadolinium gallium garnet," *J. Appl. Phys.*, vol. 41, pp. 2247–2248, 1970.
[49] H. J. McSkimin, "Measurement of elastic constants at low temperatures by means of ultrasonic waves—Data for silicon and germanium single crystals, and for fused silica," *J. Appl. Phys.*, vol. 24, pp. 988–997, Aug. 1953.
[50] N. G. Einspruch and P. Csavinszky, "Electronic effect in the elastic constant c' of silicon," *Appl. Phys. Lett.*, vol. 2, pp. 1–3, Jan. 1963.
[51] P. Csavinszky and N. G. Einspruch, "Effect of doping on the elastic constants of silicon," *Phys. Rev.*, vol. 132, pp. 2434–2440, Dec. 1963.
[52] L. J. Bruner and R. W. Keyes, "Electronic effect in the elastic constants of germanium," *Phys. Rev. Lett.*, vol. 7, pp. 55–56, July 1961.
[53] G. L. Bir and A. Tursunov, "Effect of holes on the elastic constants of germanium," *Sov. Phys.—Solid State*, vol. 4, pp. 1925–1927, Mar. 1963.
[54] J. Kushibiki and A. Tada, "Ultrasonic micro-spectroscopy characterization of silica glasses," *Tech. Rep. IEICE*, vol. US99-67, pp. 1–8, Dec. 1999.
[55] J. Kushibiki, I. Takanaga, M. Arakawa, and T. Sannomiya, "Accurate measurements of the acoustical physical constants of $LiNbO_3$ and $LiTaO_3$ single crystals," *IEEE Trans. Ultrason., Ferroelect., Freq. Contr.*, vol. 46, pp. 1315–1323, Sep. 1999.
[56] J. Kushibiki, I. Takanaga, and S. Nishiyama, "Accurate measurements of the acoustical physical constants of synthetic α-quartz for SAW devices," *IEEE Trans. Ultrason., Ferroelect., Freq. Contr.*, vol. 49, pp. 125–135, Jan. 2002.

Jun-ichi Kushibiki (M'83) was born in Hirosaki, Japan on November 23, 1947. He received the B.S., M.S., and Ph.D. degrees in electrical engineering from Tohoku University, Sendai, Japan in 1971, 1973, and 1976, respectively.

In 1976, he became a research associate at the Research Institute of Electrical Communication, Tohoku University. In 1979, he joined the Department of Electrical Engineering, Faculty of Engineering, Tohoku University, where he was an associate professor from 1988 to 1993 and became a professor in 1994. He has been studying ultrasonic metrology, especially acoustic microscopy and its applications, and has established a method of material characterization by line-focus-beam acoustic microscopy. He also has been interested in biological tissue characterization in the higher frequency range, applying both bulk and acoustic microscopy techniques.

Dr. Kushibiki is a fellow of the Acoustical Society of America, and member of the Institute of Electronics, Information and Communication Engineers of Japan; the Institute of Electrical Engineers of Japan; the Acoustical Society of Japan; and the Japan Society of Ultrasonics in Medicine.

Mototaka Arakawa (M'00) was born in Sendai, Japan on January 19, 1971. He received the B.S., M.S., and Ph.D. degrees in electrical engineering from Tohoku University, Sendai, Japan in 1993, 1995, and 2000, respectively.

In 2000, he became COE Research Fellow at the Research Institute of Electrical Communication, Tohoku University. In 2001, he became a research associate at the Department of Electrical Engineering, Faculty of Engineering, Tohoku University. His research interests include developments of the measurement methods of elastic constants of solid materials and of the calibration method of the line-focus-beam acoustic microscopy system.

Dr. Arakawa is a member of the Acoustical Society of Japan and the Institute of Electronics, Information, and Communication Engineers of Japan.

Ryoichi Okabe was born in Hakodate, Japan, on October 7, 1976. He received the B.S. degree in electrical engineering from Tohoku University, Sendai, Japan, in 2000.

He currently is studying toward the M.S. degree at Tohoku University. His research interests include developments of the measurement methods of acoustic properties of solid materials.

Mr. Okabe is a student member of the Acoustical Society of Japan.